J. Biochem. **136**, 221–231 (2004)
DOI: 10.1093/jb/mvh115

Biochemical Characterization of TT1383 from *Thermus thermophilus* Identifies a Novel dNTP Triphosphohydrolase Activity Stimulated by dATP and dTTP

Naoyuki Kondo[1], Seiki Kuramitsu[1,2] and Ryoji Masui[1,2,*]

[1]Department of Biology, Graduate School of Science, Osaka University, Toyonaka 560-0043; and [2]RIKEN Harima Institute at SPring-8, 1-1-1 Kouto, Mikazuki-cho, Sayo, Hyogo 113-0033

Received April 1, 2004; accepted May 31, 2004

The HD domain motif is found in a superfamily of proteins in bacteria, archaea and eukaryotes. A few of these proteins are known to have metal-dependant phosphohydrolase activity, but the others are functionally unknown. Here we have characterized an HD domain-containing protein, TT1383, from *Thermus thermophilus* HB8. This protein has sequence similarity to *Escherichia coli* dGTP triphosphohydrolase, however, no dGTP hydrolytic activity was detected. The hydrolytic activity of the protein was determined in the presence of more than two kinds of deoxyribonucleoside triphosphates (dNTPs), which were hydrolyzed to their respective deoxyribonucleosides and triphosphates, and was found to be strictly specific for dNTPs in the following order of relative activity: dCTP > dGTP > dTTP > dATP. Interestingly, this dNTP triphosphohydrolase (dNTPase) activity requires the presence of dATP or dTTP in the dNTP mixture. dADP, dTDP, dAMP, and dTMP, which themselves were not hydrolyzed, were nonetheless able to stimulate the hydrolysis of dCTP. These results suggest the existence of binding sites specific for dATP and dTTP as positive modulators, distinct from the dNTPase catalytic site. This is, to our knowledge, the first report of a non-specific dNTPase that is activated by dNTP itself.

Key words: HD domain, dNTP, dNTPase, dGTPase, triphosphohydrolase.

Abbreviations: CD, circular dichroism; dA, deoxyadenosine; dC, deoxycytidine; dGTPase, deoxyguanosine triphosphate triphosphohydrolase; dN, deoxyribonucleoside; (d)NDP, (deoxy)ribonucleoside diphosphate; dNK deoxyribonucleoside kinase; (d)NMP, (deoxy)ribonucleoside monophosphate; (d)NTP, (deoxy)ribonucleoside triphosphate; dT, deoxythymidine; IPTG, isopropyl-β-D(–)-thiogalactopyranoside; PPPi, inorganic triphosphate; RNR, ribonucleotide reductase; TTHB8, *Thermus thermophilus* HB8.

More than 160 genomes have been completely sequenced. One goal of these genome projects is to identify the molecular and cellular functions of all proteins encoded by open reading frames (ORFs) in genomes. Function can be assigned for two thirds of these putative proteins on the basis of sequence homology to already characterized proteins from other genomes. However, there is some uncertainty in such functional assignment because some ORFs are annotated exclusively based on the presence of a characteristic sequence motif. The same functional domain can be used either as a catalytic or non-catalytic component (*1*). It has been assumed that overall sequence similarity reflects functional similarity, but even this assumption is not necessarily the case (*2*, *3*). Experimental studies to infer protein function must be performed individually in a similar manner as for hypothetical (functionally unknown) proteins with such broadly predicted functions.

In the genome of *Thermus thermophilus* HB8 (TTHB8), an extremely thermophilic Gram-negative eubacterium (*4*), function can be assigned for two-thirds of the ORFs mainly based on sequence similarity. Several approaches other than sequence comparison have been used to predict gene function, such as the gene disruption, protein-protein network analysis, and protein structural analysis. The proteins of TTHB8 are also one of the targets of the RIKEN Structural Genomics Initiative (*5*). Although the above approaches, especially the determination of 3D structures, have led to functional assignments for some hypothetical proteins, the molecular functions of most putative proteins are still unclear.

We have studied TTHB8 proteins involved in DNA repair and nucleotide metabolism (*6–11*). To discover novel enzymes involved in these processes, we have also been analyzing functionally unknown proteins containing nucleotide-binding motifs among broadly annotated proteins. In this study, we focus on the TT1383 gene product of TTHB8. As its primary structure is similar to dGTP triphosphohydrolase (dGTPase) (*12*), TT1383 is annotated dGTPase. However, the sequence similarity is relatively low and restricted to the region around an HD domain, a nucleotide-binding motif present in a large family of functionally distinct proteins (*13*). Here we isolated the TT1383 gene product and investigated its biochemical properties. Detailed analysis of the biochemical activity leads to the conclusion that TT1383 is not a dGTPase, but a novel dNTP triphosphohydrolase with a unique activation mechanism.

*To whom correspondence should be addressed. Tel: +81-6-6850-5434, Fax: +81-6-6850-5442, E-mail: rmasui@bio.sci.osaka-u.ac.jp

Table 1. **Activity of various dNTP mixtures, each at a concentration of 50 μM, at 37°C for 1 h in buffer E (see "MATERIALS AND METHODS").**

Entry	Number of mixed dNTPs	The contents of dNTP mix					Proportion of products (%)[a]				
		dATP	dGTP	dTTP	dCTP	dUTP	dA	dG	dT	dC	dU
1	5	+	+	+	+	+	31	58	45	96	23
2	4	–	+	+	+	+	–	19	9	45	12
		+	–	+	+	+	32	–	46	96	25
		+	+	–	+	+	11	11	–	57	13
		+	+	+	–	+	34	69	49	–	27
		+	+	+	+	–	29	61	42	95	–
3	3	+	+	+	–	–	33	63	45	–	–
		+	–	+	–	+	33	–	38	–	26
		+	–	+	+	–	35	–	41	96	–
		+	–	–	+	+	12	–	–	64	16
		+	+	–	–	+	11	34	–	–	15
		+	+	–	+	–	3	9	–	13	–
		–	+	–	+	+	–	0	–	0	0
4	2	+	–	+	–	–	31	–	42	–	–
		+	–	–	–	+	12	–	–	–	15
		+	–	–	+	–	3	–	–	12	–
		+	+	–	–	–	5	9	–	–	–
5	1	+	–	–	–	–	0	–	–	–	–
		–	+	–	–	–	–	0	–	–	–
		–	–	+	–	–	–	–	0	–	–
		–	–	–	+	–	–	–	–	0	–
		–	–	–	–	+	–	–	–	–	0

[a]The product proportion was determined by the relative composite concentrations of reactant and products.

MATERIALS AND METHODS

Expression and Purification—Escherichia coli BL21(DE3) (Novagen) was transformed with pET-11a/tt1383, supplied by the "Structural-Biological Whole Cell Project" (*5*). Transformant were grown at 37°C in 1.5 liter of YT medium containing 50 μg/ml ampicillin. When the cell density reached 5×10^8 ml^{-1}, isopropyl-β-D(–)-thiogalactopyranoside (IPTG) at a final concentration of 1 mM was added to induce expression. After additional incubation for 5 h, the cells were harvested and stored at –80°C.

Frozen cells (6 g) were thawed, suspended in 50 ml of buffer A (50 mM Tris-HCl, 5 mM EDTA, and 5 mM β-mercaptoethanol, pH 8.0), and then disrupted by ultrasonication for 10 min on ice. The cell lysate was heated at 70°C for 10 min to remove endogenous *E. coli* proteins. After cooling in ice water, the lysate was centrifuged at 10,000 × *g* for 90 min at 4°C. The supernatant was loaded onto a Super-Q Toyopearl (Tosoh) column (bed volume: 50 ml) equilibrated with buffer A. The column was then washed with 150 ml of buffer A and eluted with a linear gradient of NaCl from 0 to 1 M in buffer A, with a total elution volume of 300 ml. The fractions that eluted at about 500 mM NaCl were dialyzed against buffer B (10 mM potassium phosphate, 1 mM EDTA, and 1 mM β-mercaptoethanol, pH 7.8) and loaded onto a hydroxylapatite (nacalai tesque) column (bed volume: 50 ml) equilibrated with buffer B. The flow-through fraction was collected and separated on a Superdex 200 HR 10/30 column (Amersham Bioscience) equilibrated with buffer C (50 mM Tris-HCl and 100 mM KCl, pH 8.0) using the ÄKTA system (Amersham Bioscience). Sample purity was confirmed by SDS-PAGE. The protein concentration was determined by measuring absorbance at 278 nm using an extinction coefficient ε_{278} of 30,765 M^{-1} (*14*).

Circular Dichroism (CD) Measurements—CD spectra in the far-UV region from 200 nm to 250 nm were obtained at 25°C with a Jasco spectropolarimeter, J-720W on 5 μM enzyme in buffer D (10 mM potassium phosphate, 100 mM KCl, and 10 mM magnesium acetate, pH 7.8). Thermostability was investigated by recording the molar ellipticity at 222 nm from 15°C to 95°C under the same conditions as above.

Size Exclusion Chromatography—The protein was applied to a Superdex 200 HR 10/30 column and eluted with buffer C. The apparent molecular mass was estimated by comparing its retention time with those of molecular mass markers (Sigma).

Assays for Enzyme Activity—All enzyme reactions were performed at 37°C in buffer E (50 mM Tris-HCl, 100 mM KCl and 10 mM $MgCl_2$, pH 7.5) with 1 μM enzyme, and stopped by adding 0.5 M EDTA to a final concentration of 20 mM. The reaction time was 1 hr in the experiments shown in Table 1, Figs. 4 and 5, and 10 min to measure the initial velocity in the experiments shown in Figs. 6 and 7. On both time scales, linearity between activity and reaction time was confirmed. After the reaction, the protein was removed using a VIVASPIN concentrator (Vivascience), and the filtered solution was analyzed by ion-pair reverse-phase chromatography (*15*) using a CAPCELL PAK C18 column (Shiseido Fine Chemicals) on the ÄKTA system. The column was equilibrated with buffer F (20 mM sodium phosphate [pH 7.0], 5 mM tetra *n*-butylammonium phosphate, and 5% methanol) and eluted with a linear gradient of methanol from

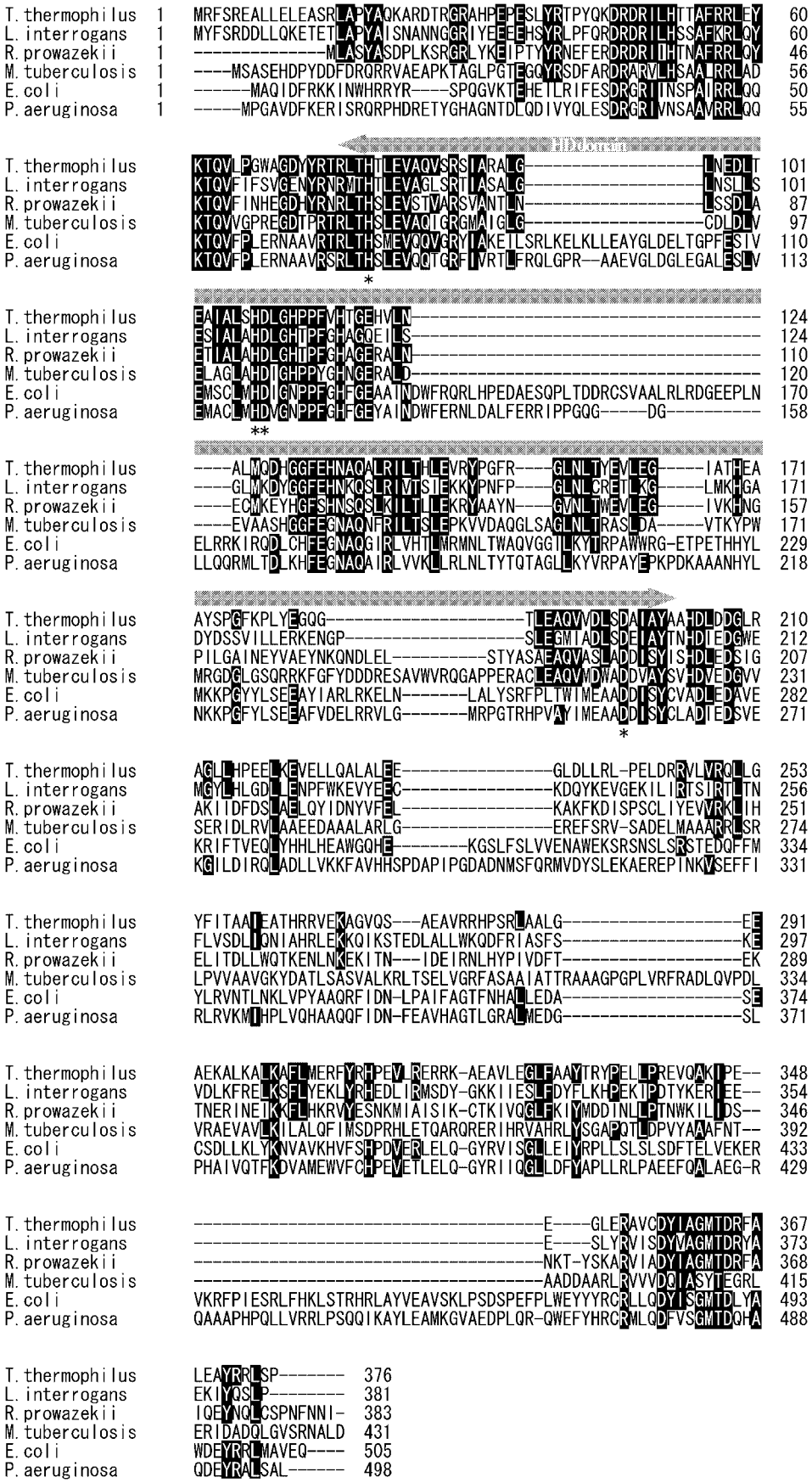

Fig. 1. **Multiple sequence alignment of *T. thermophilus* TT1383 with dGTP triphosphohydrolase homologues.** Sequences are obtained from *Leptospira interrogans* (NCB Accession AAN49473), *Rickettsia prowazekii* (Q9ZE82), *Mycobacterium tuberculosis* (NP_216860), *Escherichia coli* (AAA23679), and *Pseudomonas aeruginosa* (Q9I4L1). When more than three amino acid residues are identical to TT1383, the residues are indicated by white letters on black. The gray arrow over the sequences represents the HD domain. Completely conserved residues in the HD domain are indicated by asterisks at below the sequences.

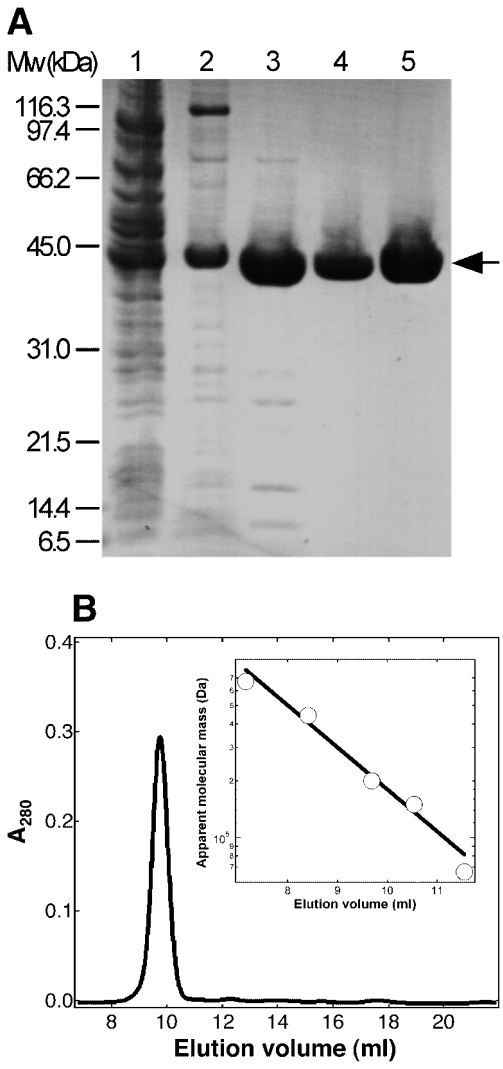

Fig. 2. **Overexpression and purification of TT1383.** (A) Overexpressed and purified TT1383. SDS-PAGE was carried out using a 10–20% gradient polyacrylamide gel. Positions of molecular mass markers are indicated on the left. Samples are: lane 1, total cell extract; lane 2, supernatant after heat treatment; lanes 3, 4, and 5, Super-Q Toyopearl, hydroxylapatite and Superdex 200 HR chromatography fractions, respectively. The arrow indicates the position of TT1383. (B) Oligomeric state. Size exclusion chromatography was performed for 5 μM protein in buffer C (50 mM Tris-HCl [pH 8.0] and 100 mM KCl). inset: Estimation of the apparent molecular mass. The molecular size markers were thyroglobulin (669,000 Da), apoferritin (443,000 Da), β-amylase (200,000 Da), alcohol dehydrogenase (150,000 Da), and bovine serum albumin (66,000 Da).

5 to 60%. Products and reactants were quantified by measuring their absorbance at 260 nm. The approximate extent of the reaction was quantified by determining the relative composite concentrations of substrates and products. When the peaks of some dNTPs overlapped, quantification was carried out by superimposing calibration curves for each deoxyribonucleoside upon the absolute integrated value of each product peak.

Mass Spectrometry—After protein removal, the reaction mixture was loaded onto an Atlantis column (Waters) equilibrated with buffer G (10 mM ammonium formate [pH 3]). The respective products were fractionated, dried in an evaporator (Sakuma), dissolved in a 1:1 mixed solvent of pure water and methanol, and analyzed by an LCQ mass spectrometer (ThermoFinnigan) on positive mode.

Kinetic Analysis—Assuming a Michaelis-Menten type equation, Eqs. 1 and 2, curve fitting was performed for the data in double reciprocal plots (Fig. 7) based on Eq. 3.

$$\mathrm{E} + \mathrm{S} \underset{k_{-1}}{\overset{k_1}{\rightleftharpoons}} \mathrm{ES} \xrightarrow{k_2} \mathrm{E} + \mathrm{P} \quad (1)$$

$$v_0 = V_{\max}^{\mathrm{app}}[\mathrm{S}]/(K_{\mathrm{m}}^{\mathrm{app}} + [\mathrm{S}]) \quad (2)$$

where $K_{\mathrm{m}}^{\mathrm{app}} = (k_1 + k_2)/k_1$, $V_{\max}^{\mathrm{app}} = k_2[\mathrm{E}]_0$.

$$1/v_0 = K_{\mathrm{m}}^{\mathrm{app}} / V_{\max}^{\mathrm{app}} [\mathrm{S}] + 1/ V_{\max}^{\mathrm{app}} \quad (3)$$

RESULTS

Sequence Analysis—A functionally unknown open reading frame, TT1383 (DDBJ/EMBL/GenBank accession No. AB107661; project code 1383), encoded in the TTHB8 genome was 1,128 bp in length. Search using the BLAST algorithm (*16*) indicated that the amino acid sequence of this gene product (376 aa, Mw = 42,600) most resembles that of bacterial dGTPases (*12*) and retains an HD domain motif (*13*). The HD domain, in which two histidine and two aspartate residues are conserved, is likely to be linked to metal-dependent phosphohydrolase activity and is found in diverse proteins involved in nucleotide metabolism. Figure 1 shows a multiple sequence alignment of TT1383 and several putative dGTPase homologues. The N-terminal region containing the HD domain is highly conserved among all proteins, but the *E. coli* and *Pseudomonas aeruginosa* protein sequences require many gaps to be inserted for optimal alignment. Such gaps in the *E. coli* and *P. aeruginosa* protein sequences were also observed in the C-terminal region.

Among bacterial dGTPase homologues, dGTPase activity has been experimentally verified only for those from *Enterobacteriaceae* (*17*), which include *E. coli* (*12*) and *Shigella boydii* (*18*), a close relative of *E. coli*. Of the bacteria listed in Fig. 1, only *E. coli* belongs to the *Enterobacteriaceae* family. Even though the amino acid sequence of the *P. aeruginosa* dGTPase homologue most resembles that of *E. coli*, it has already been shown that the *P. aeruginosa* homologue does not have dGTPase activity (*17*). These results suggest that such dGTPase homologues, distributed among many kinds of eubacteria, possess a variety of unknown functions.

Overproduction and purification of TT1383—To characterize the TT1383 gene product, we overexpressed TT1383 in *E. coli* under the control of the IPTG-inducible T7 promoter. After heat treatment of the cell lysate at 70°C, the TT1383 gene product was isolated through three steps of column chromatography: anion exchange, hydroxylapatite, and size exclusion (Fig. 2A).

Biophysical Properties—The oligomeric state of the enzyme was investigated by size exclusion chromatography. The elution profile showed a single peak (Fig. 2B) with an apparent molecular mass corresponding to about 210,000 Da (Fig. 2B, inset). As the molecular weight of a

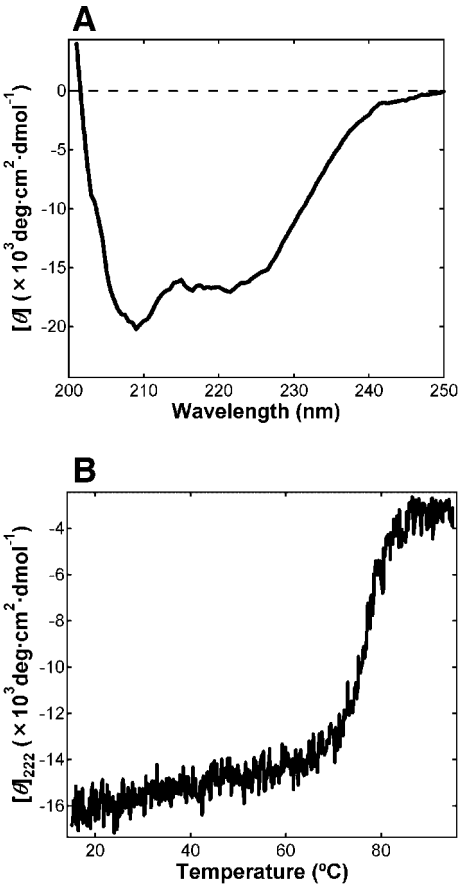

Fig. 3. **Secondary structure.** (A) Far-UV CD spectrum. Measurement was performed at 25°C using 5 μM enzyme in buffer D (10 mM potassium phosphate, 100 mM KCl, and 10 mM magnesium acetate). (B) Thermostability. Conditions were the same as those in (A) except for temperature.

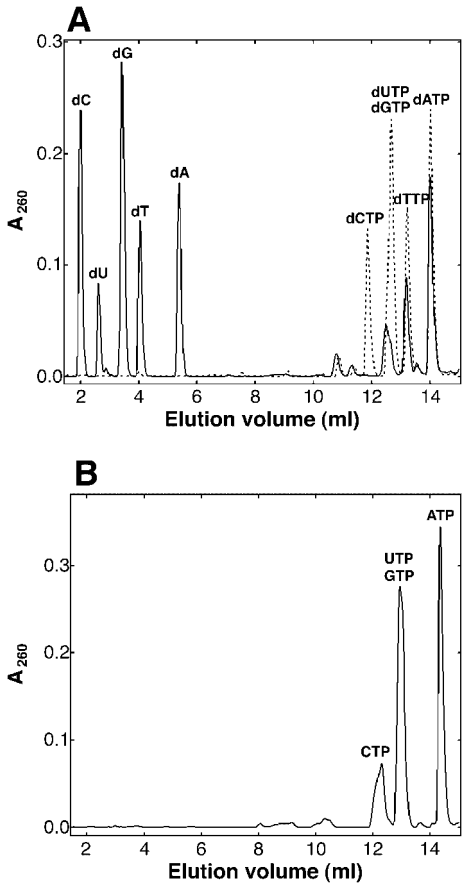

Fig. 4. **Hydrolysis activity for dNTP (A) and NTP (B) mixtures.** Reaction mixtures contained 1 μM enzyme, 50 μM dNTPs, 50 mM Tris-HCl and 100 mM KCl, pH 7.5. The reactions were performed at 37°C for 1 h, and the reactants were analyzed by ion-pair chromatography (see the text for details). Solid and dotted lines represent the chromatograms for reactions in the presence and absence, respectively, of 10 mM $MgCl_2$.

monomer of this protein was calculated from its amino acid sequence to be 42,600, the native protein is likely to form a pentamer in solution.

The far-UV CD spectrum (Fig. 3A) shows negative maxima at 208 and 222 nm, indicating that this enzyme contains helical structures. In addition, the thermostability of the secondary structure was examined by measuring the ellipticity at 222 nm (Fig. 3B). The results indicate that the protein is stable to about 70°C.

Searching for Activity—Because it possesses a certain degree of sequence similarity to dGTPases and contains an HD domain, which implies a metal-dependent phosphohydrolase activity (*13*), we first examined the dNTPase activity of the TT1383 protein for each dNTP in the presence of Mg^{2+}, but detected no hydrolytic activity (Table 1, Entry 5). Even for high concentrations of dNTPs, up to 2 mM, no hydrolysis was detected. Every NTP, NDP, NMP, dNDP, dNMP, cyclic NMP, single-stranded DNA and double-stranded DNA yielded the same results as those obtained for dNTPs (data not shown). Next, a dNTP mixture (dATP, dTTP, dGTP, dCTP, and dUTP) was used as a substrate, in the presence of Mg^{2+}. Unexpectedly, the peak areas corresponding to all of the dNTPs decreased, and five peaks appeared at earlier retention times (Fig. 4A, solid line). Comparison with the retention times for synthetic dNDPs, dNMPs, and deoxyribonucleosides revealed that these peaks corresponded to their respective deoxyribonucleosides. Mass spectrometric analysis of the products confirmed that the molecular weights were equal to those of the deoxyribonucleosides corresponding to each dNTP (data not shown). Even during the initial phases of the reaction, no intermediates were detected. Therefore, the hydrolytic activity is consistent with that of a typical triphosphohydrolase; that is, dNTP + H_2O → deoxyribonucleoside (dN) + inorganic triphosphate (PPPi).

A mixture of four NTPs (ATP, GTP, CTP and UTP) in the presence of Mg^{2+} did not result in hydrolysis of any of the substrates (Fig. 4B); even in a reaction containing a mixture of five dNTPs and four NTPs, the dNTPs were selectively hydrolyzed (data not shown). These results suggest that this enzyme is specific for dNTPs. The order of conversion rate was dCTP (96) > dGTP (58) > dTTP (45) > dATP (31) > dUTP (21), as shown in Table 1, Entry 1. In the absence of Mg^{2+}, no hydrolysis was observed (Fig. 4A, dotted line). This Mg^{2+} dependence reflects a general feature of the HD domain, which is known to encode a metal-dependent phosphohydrolase activity (*13*).

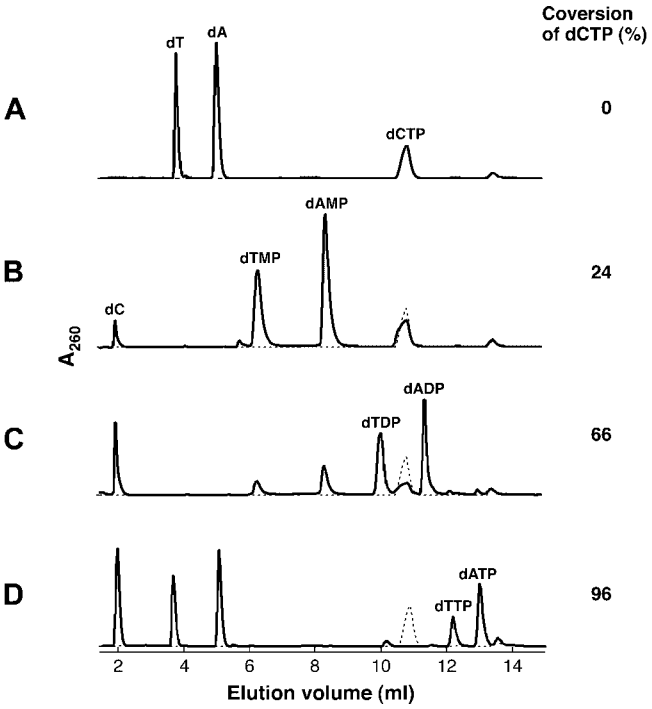

Fig. 5. **Effect of deoxyadenosine and deoxythymidine derivatives on dCTP hydrolysis.** The measurements were performed under the conditions described in Fig. 4 in the presence of $MgCl_2$, except for substrates (and activators). Reaction mixtures contained 50 μM dCTP as a substrate and the following nucleosides and nucleotides at each 50 μM as activators: A, dA and dT; B, dAMP and dTMP; C, dADP and dTDP; and D, dATP and dTTP. Dotted lines represent elution profiles in the absence of activator. Solid lines represent elution profiles in the presence of activator. The values noted to the right side of each figure represent dCTP hydrolysis rates

Effect of dNTP Combination on Activity—The TT1383 gene product does not hydrolyze single dNTPs but does hydrolyze a mixture of five dNTPs. To investigate which dNTP is required for activity, various combinations of dNTPs were used as substrates. First, mixtures of four dNTPs were investigated (Table 1, Entry 2). dNTPase activity was detected in all cases with preferences for specific dNTP combinations. dCTP showed the highest extent of conversion, followed by dGTP, dTTP, dATP, and dUTP. This order of dNTP specificity was the same as that of the mixture of five dNTPs. This hierarchy of specificity, as well as the absolute conversion rates for each species, was maintained in the absence of dGTP, dCTP or dUTP: dA ≈ 30, dG ≈ 60, dT ≈ 45, dC ≈ 95 and dU ≈ 25. In contrast, hydrolysis in the absence of dATP or dTTP was significantly slower than that observed in the former cases.

For mixtures of three dNTPs, the enzyme also showed lower conversion rates in the absence of dATP or dTTP. Entry 3 in Table 1 shows the results of mixtures containing dATP. In the presence of both dATP and dTTP, the rate of dNTP hydrolysis was the highest of all the three-component mixtures, corroborating the results obtained for the four- and five-component mixtures, shown in Entries 1 and 2, respectively. In the presence of dATP, but not dTTP, dNTP hydrolysis slowed universally. Entry 3 in Table 1 also shows that in the absence of both dATP and dTTP, hydrolysis did not occur.

Finally, mixtures of two dNTPs were investigated. Similar to the results described above, in the absence of both dATP and dTTP, no reaction took place (data not shown). Entry 4 in Table 1 shows the reactivity for combinations of two dNTPs including dATP. The combination of dATP and dTTP exhibited the highest activity. The conversion in this case was almost the same as that obtained in the presence of both dATP and dTTP in Entries 1, 2, and 3. The dATP/dUTP pair followed in activity, whereas the dATP/dCTP and dATP/dGTP pairs showed considerably lower activity. In total, examining various dNTP substrate combinations, the data suggest that dATP and dTTP promote dNTPase activity and, at the same time, can be substrates of the enzyme, and that the other three dNTPs tested are not essential for promoting activity, but can be substrates, with two (dGTP and dCTP) preferable to dATP and dTTP as substrates.

Effects of dATP and dTTP Analogues on Activity—To characterize further the effects of dATP and dTTP on enzymatic activity, we examined whether dATP and dTTP analogues could promote dNTP hydrolysis (Fig. 5). This effect was measured using dCTP, which was the most reactive substrate (Table 1). In the presence of deoxyadenosine (dA) and deoxythymidine (dT) together, dCTP was not hydrolyzed (Fig. 5A). As phosphate groups were added, however, the rate of dCTP hydrolysis increased (Fig. 5B–D). The order of the promotion effect was: dATP/dTTP > dADP/dTDP > dAMP/dTMP (> dA/dT). It should be mentioned that for dAMP/dTMP and dADP/dTDP, no product peak other than deoxycytidine (dC) was detected (In Fig. 5C, the peaks corresponding to dAMP and dTMP were contaminants among the dADP and dTDP substrates, and not products). This is in contrast to the case of dATP and dTTP, which were themselves hydrolyzed.

These results strongly suggest that dATP/dTTP and their analogues act as activators of this dNTPase activity. The failure of the enzyme to hydrolyze dADP/dTDP or dAMP/dTMP (Fig. 5B and C) suggests the existence of an activator recognition site that specifically recognizes dA or dT derivatives but does not hydrolyze them. In addition, phosphate groups are thought to be required for activator function because dA and dT provide no activation, and the presence of larger numbers of phosphate groups leads to higher activity. When ATP/dTTP was included instead of dATP/dTTP, the dCTPase activity was 15% as the conversion of dCTP, illustrating the importance of the deoxyribose moiety in the activator molecules.

Effect of dNTP Ratio—Next, the hydrolysis of dATP and dTTP was studied with their total concentration constant. Figure 6A shows the dATPase activity at various dATP–dTTP ratios at total concentrations of 100, 200, and 500 μM. Although dATP when present alone in the absence of dTTP is not hydrolyzed at any concentration (also see Table 1, Entry 5), dATPase activity in the presence of dTTP increases in proportion to dATP concentration. Similarly, Fig. 6B indicates an increase in dTTPase activity in proportion to dTTP concentration. Figure 6C shows the total dNTPase activity, which in these cases corresponds to the sum of the dATPase and dTTPase

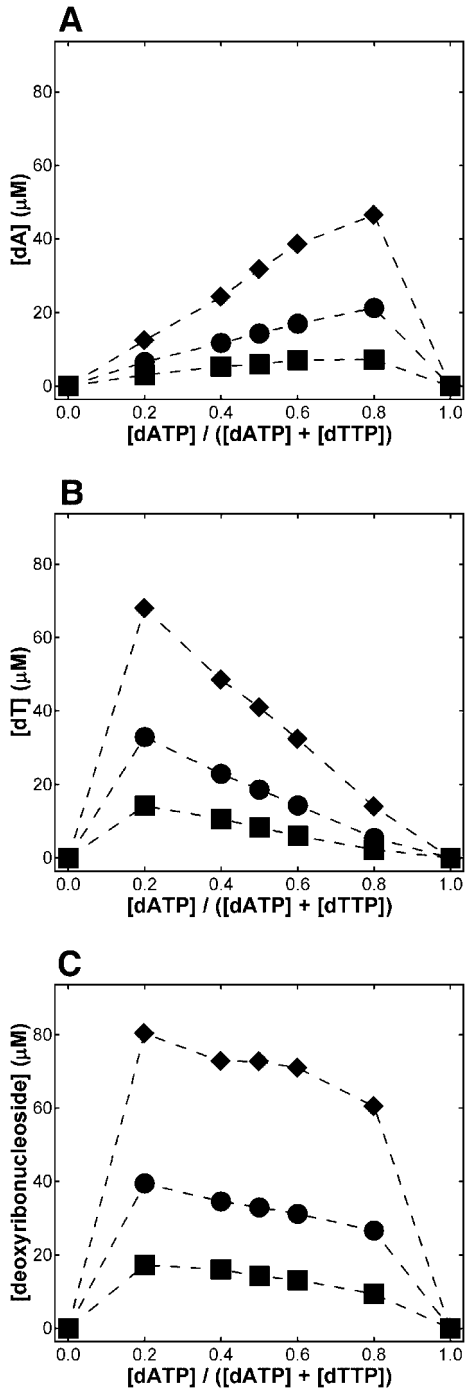

Fig. 6. **Effect of the ratio of activator concentrations on dNTPase activity.** The dATPase and dTTPase activities were measured at constant total dNTP concentrations at 37°C for 10 min. The reaction mixtures contained 1 μM enzyme, dATP, dTTP, 50 mM Tris-HCl, 100 mM KCl, and 10 mM $MgCl_2$, pH 7.5. The dNTP concentrations were 100 μM (filled squares), 200 μM (filled circles), or 500 μM (filled diamonds). A, B, and C show the amounts of dA (A), dT (B), and the sum of dA and dT (C).

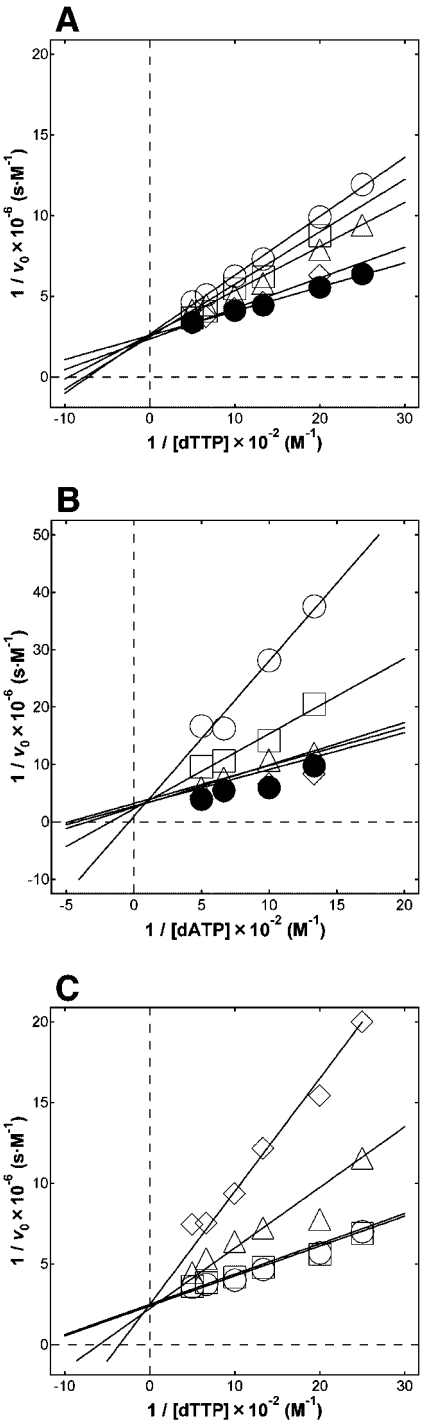

Fig. 7. **Effect of dATP and dTTP concentrations on enzyme activity.** Measurements were performed under the conditions described in Fig. 6, except for nucleotide concentration. (A) dTTPase activity at low concentrations of dATP in excess dTTP (more than 400 μM). The dATP concentrations were 1 μM (open circles), 1.5 μM (open squares), 2 μM (open triangles), 5 μM (open diamonds), and 7 μM (filled circles). (B) dATPase activity at low concentrations of dTTP in excess dATP (more than 750 μM). The dTTP concentrations were 2 μM (open circles), 5 μM (open squares), 10 μM (open triangles), 30 μM (open diamonds), and 50 μM (filled circles). (C) dTTPase activity at high concentrations of dATP in excess dTTP (more than 400 μM). The dATP concentrations were 10 μM (open circles), 100 μM (open squares), 500 μM (open triangles), and 1 mM (open diamonds).

activities. These data indicate that at least 20 μM dATP or dTTP is sufficient to activate the hydrolysis reaction.

Cooperativity of dNTPase Activators—To obtain clues about the mechanism by which dATP or dTTP activates the dNTPase activity, titrations of dTTP at various con-

centrations of dATP and vice versa were performed. The data were fitted to Eq. 3. At low dATP concentrations (up to 7 μM) and excess dTTP concentration (more than 400 μM) (Fig. 7A), the V_{max}^{app}, corresponding to the *y*-intercept, was constant (approximately 0.4 μM·s^{-1}), whereas the K_m^{app}/V_{max}^{app} , corresponding to the slope of each line, decreased in proportion to dATP concentration. This suggests that dTTPase activity is activated by dATP. The observation that the fitted lines for the respective dATP concentrations showed a crossing point on the ordinate is consistent with an ordered mechanism with sequential steps for cooperativity in which the activator molecule is dATP (*19*).

Similarly, the dATPase activity increased with dTTP concentrations up to 30 μM in excess of dATP (more than 750 μM): the V_{max}^{app} was constant (approximately 0.4 μM·s^{-1}) and the slope changed (Fig. 7B). The concentration of dTTP required for maximal activity, however, was considerably higher than that of dATP. This difference suggests that dATP has a higher affinity for the activator binding site than does dTTP. Also in this case, dTTP seems to activate dATPase activity with an ordered mechanism as the fitted lines for the respective dTTP concentrations had a crossing point on the ordinate. The activator actions (Fig. 7, A and B) can be summarized as follows: dATP decreases the K_m^{app} of dTTP, and dTTP decreases the K_m^{app} of dATP. At zero dATP, the K_m^{app} of dTTP approaches infinity, indicating no binding. Also at zero dTTP, the K_m^{app} of dATP approaches infinity indicating no binding. These results indicate ordered binding with the activator preceding the substrate.

At high concentrations of both dATP (more than 500 μM) and dTTP (more than 400 μM), on the other hand, dTTPase activity was inhibited by dATP in a manner consistent with competitive inhibition as constant V_{max}^{app} (approximately 0.3 μM·s^{-1}) and an increase in slope were observed with a crossing point on the ordinate (Fig. 7C). This inhibition suggests that dATP competes with dTTP for the catalytic site independent of their binding to the activator recognition site.

DISCUSSION

The most striking result of this study is the finding that the dNTPase activity of TT1383 was observed only with a mixture of dNTPs, and not with single dNTPs. Insight into this complicated reaction was provided by the results presented in Table 1. Table 1, Entry 3, the results obtained when mixtures of three dNTPs were used, clearly demonstrates that mixtures containing both dATP and dTTP yield the highest activity, while those without dATP and dTTP demonstrate less activity. Furthermore, Table 1, Entry 4, which illustrates the results obtained using mixtures of two dNTPs, demonstrates a clear hierarchy of substrate preference in the presence of dATP: dATP/dTTP > dATP/dUTP > dATP/dGTP > dATP/dCTP. This result confirms the importance of dATP and dTTP for enzymatic activity. It should be noted, however, that even in the absence of dATP, the presence of dTTP was sufficient for activity (Table 1, Entry 2), indicating that at least one of dATP and dTTP is absolutely necessary. Therefore, we have come to the conclusion that this enzyme requires at least two dNTPs, one of which must be either dATP or dTTP, and that once activated, this enzyme specifically hydrolyzes any dNTP. To our knowledge, this is the first report describing a dNTPase with such a complicated mechanism.

Next, we tried to construct a model for the enzymatic reaction. The results shown in Figs. 5 and 7A, B suggest that the enzyme has separate activator recognition and catalytic sites. This notion is supported by the results shown in Table 1, which suggest that the order of effectiveness of a dNTP species as an activator, dATP/dTTP > dATP/dUTP > dATP/dGTP > dATP/dCTP, does not coincide with its specificity as hydrolyzed substrate, dCTP > dGTP > dTTP > dATP > dUTP. Based on the presence of two sites for dNTP, the simplest model for the reaction, which illustrates ordered binding with the activator preceding the substrate, can be proposed as Scheme 1.

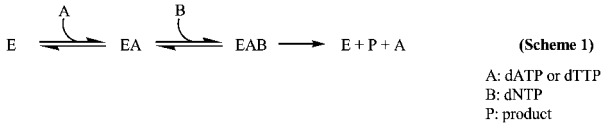

Though this model satisfies the presence of two separate sites, it cannot explain why the enzyme has its highest dNTPase activity in the presence of both dATP and dTTP (Table 1). Therefore, this simple model is unlikely to be correct.

To improve the model, we postulated the presence of two activator recognition sites in the enzyme, because the coexistence of dATP and dTTP induced the highest dNTPase activity. A modified model is presented in Scheme 2.

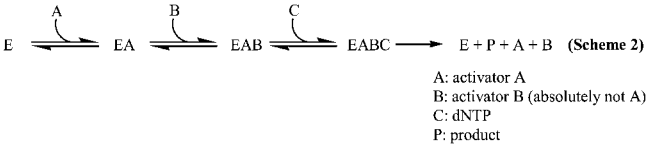

In Scheme 2, dATP or dTTP is suitable as activator A, while dNTP, which is absolutely not activator A, is suitable as activator B. If these conditions are met, the complicated mechanism of activation reported in this paper can be explained by this model. The findings that the dNTPase activity is observed only in the presence of more than two dNTPs containing dATP "or" dTTP and that coexistence of dATP and dTTP induces the highest dNTPase activity (Table 1) can be explained by this model if the first activator-binding site is highly specific for dATP or dTTP, and second activator-binding site has moderate specificity for any dNTP. In addition, the difference in the specificity between dNTPs as activators and dNTPs as substrates can be explained by the existence of site C as a catalytic site. As this model is the simplest and the most reasonable of the models we have considered, we used it to analyze the kinetic data of the reaction involving dATP and dTTP (Fig. 7).

To characterize the parameters of this scheme from the results obtained in Fig. 7, we constructed a modified scheme in which the enzyme has two activator recognition sites and a separate catalytic site as Scheme 3.

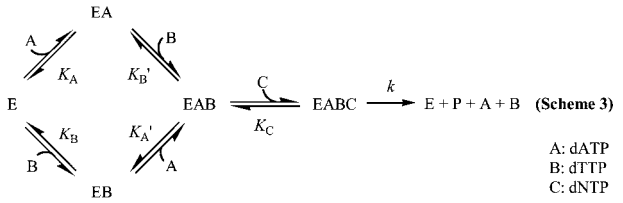

In Scheme 3, K_A, K_A', K_B, K_B' and K_C are the dissociation constants for the respective binding steps under the assumption of rapid equilibrium, and k is the rate constant of the irreversible catalytic step. The reaction rate, v, was calculated using these parameters and Eqs. 4–7 as follows:

$$[E]_0 = [E] + [EA] + [EB] + [EAB] + [EABC] \quad (4)$$

$$K_A'K_B = K_AK_B' \quad (5)$$

$$V_{max} = k[E]_0 \quad (6)$$

$$v = k[EABC] \quad (7)$$

These equations are combined, leading to Eq. 8:

$$v = V_{max}[C]/([C] + K_C\,(K_A'K_B/[A][B] + K_B'/[B] + K_A'/[A] + 1)) \quad (8)$$

This equation can explain the results shown in Fig. 7A and B, in which dATP and dTTP stimulated dTTPase and dATPase activity, respectively, in an ordered mechanism-like manner. When dTTP is in excess, Eq. 8 simplifies to Eq. 9,

$$v = V_{max}[C]/([C] + K_C\,(K_A'/[A] + 1)) \quad (9)$$

As this equation formally corresponds to the equation of ordered mechanism, stimulation of activity by high dATP concentrations, such as that shown in Fig. 7A, can be understood in terms of this equation. Similarly, when dATP is in excess, Eq. 8 simplifies to Eq. 10,

$$v = V_{max}[C]/([C] + K_C\,(K_B'/[B] + 1)) \quad (10)$$

which describes stimulation by dTTP alone, such as that seen in Fig. 7B, and also conforms to an ordered mechanism.

The usefulness of Eq. 8 to explain the observed phenomena corroborates the validity of Scheme 3. Therefore, kinetic parameters were determined by applying Eq. 8 to the data in Fig. 7, the slope and the intercept, assuming several simplifications as follows. At high concentrations of both dATP and dTTP, Eq. 8 simplifies to $1/[A] \rightarrow 0$ and $1/[B] \rightarrow 0$ to Eq. 11.

$$v = \frac{V_{max}[C]}{[C] + K_C} \quad (11)$$

In these concentration ranges, increasing the concentration augments the effect of dNTP competition for the active site. Therefore, K_C and k were calculated for each individual dNTP in a concentration range of the other outside this range of inhibition (Fig. 7C, 100 μM dATP or Fig. 7B, 30 μM dTTP). Using K_C, Eqs. 9 and 10, K_A', and K_B' were calculated. Finally, K_A and K_B were calculated using these parameters, Eqs. 5, and 8. Inhibition constant of dATP from Fig. 7C was calculated with K_C of dTTP and Eq. 11.

Table 2. **Kinetic parameters from Eq. 8.**

Dissociation constant (μM)	
K_A	120 ± 180
K_B	1000 ± 1600
K_A'	1.1 ± 0.17
K_B'	9.3 ± 1.5
$K_C^{dATP\,a}$	2000 ± 280
$K_C^{dTTP\,a}$	620 ± 76
$K_I^{dATP\,a}$	860 ± 79
Rate constants (s^{-1})	
k_{dATP}	0.45 ± 0.037
k_{dTTP}	0.29 ± 0.15

[a]The superscript of K_C and K_I and the subscript of k represent dNTP as C in Scheme 3.

Table 2 indicates the calculated dissociation constants. The parameters in this table suggest that the affinity of dATP as an activator is stronger than that of dTTP and that the first steps of activator binding indicate higher dissociation constants than the second steps of activator binding. This dataset implies that the binding of the first activator promotes the specific binding of the second activator by allosteric conformational change of the enzyme. On the other hand, the affinities (K_C) of both nucleotides as substrates are comparable to each other as predicted by the results in Table 1, and their rate constants, k, are also similar, approximately 0.3–0.4 s^{-1}. These results about the hydrolytic reaction can support that this enzyme has low specificity for dNTPs as substrates.

The two remarkable features of the activation pattern are the requirement for more than two dNTPs and the failure of single dNTPs to be hydrolyzed. While the proposed model explains the former feature, it does not do well with the latter. In other words, this model predicts that the binding of dATPs to both activator binding sites leads to hydrolysis of dATP in the catalytic site. In practice, however, dATP alone is insufficient for activity. In both pathways of the activator binding step, the affinity of the second activator molecule is much stronger than that of the first (Table 2). Allosteric change in the enzyme structure upon binding of the first activator may be sufficient to course stronger affinity, but seems insufficient to explain the requirement for a different type of dNTP as the second activator molecule. Thus, we considered the possibility that there are interactions between two different dNTPs in the activator recognition sites, and that these act as selector for the second activator.

The well-known interaction between nucleotides is that in a DNA duplex. Interestingly, maximal activation was achieved when dATP and dTTP were present together. Therefore, we propose a speculative hypothesis that two bound activators form a Watson-Crick base pair in the binding site. In the presence of dATP, the dATPase activity was promoted in the following order: dTTP > dUTP > dGTP > dCTP, while single dATP was not hydrolyzed (Table 1). This order coincides with the order of

base-pair stability in DNA. dTTP, which shows the highest activity, is the preferred partner of dATP. dUTP, following dTTP in activity, contains a uracil moiety, which can base-pair with adenine in RNA duplexes. As for the other three dNTPs, it was reported by Kierzek *et al.* that the order of thermostability for mismatched base pairs is A-G > A-C > A-A (*20*). These data support the hypothesis that base-pairing between two bound dNTPs occurs in this enzyme. Peyret *et al.* examined the stabilities of mismatched pairs composed of two identical bases, and found that A-A was nearly equivalent in stability to T-T (*21*). Based on the above hypothesis, this report explains why single dATP and dTTP are barely hydrolyzed (Table 1, Entry 5). Therefore, we consider that in the proposed reaction model (Scheme 3), base-pairing between two dNTPs bound to activator recognition sites stimulates the catalytic reaction.

In this regard, the relationship between the oligomeric state and the reaction mechanism is of high interest because this enzyme probably exists as a pentamer. It is still uncertain whether the three dNTP binding sites premised by the proposed model exist in the same subunit or not. Some dNTP-binding enzymes are known to have complicated regulatory mechanisms. Ribonucleotide reductase (RNR) (*22*), which synthesizes dNDP from NDP, has complicated allosteric regulation mechanism caused by dNTPs and ATP. The R1 subunit of the class Ia enzyme has three regulating sites per subunit, which effect substrate specificity or activity (*22*). Deoxyribonucleoside kinase (dNK) (*23*), which phosphorylates dN to generate dNMP, is inhibited by its respective dNTP. dNTP binds to substrate binding sites to act as the bisubstrate inhibitor (*24*). Such intricate mechanisms in regulation serve to maintain the intracellular level of deoxyribonucleotides. We think the complicated (but not yet definitely solved) mechanism of the TT1383 dNTPase implies that this enzyme is concerned with some aspect of regulation of the deoxyribonucleotide metabolism, for instance, sanitization of overproduced dNTPs in replication to reduce the mutation rate. The hydrolytic style of TT1383, triphosphohydrolase-type, appears to support the connection of this regulation as the product of the reaction, deoxyribonucleoside, can not easily return to the pathway of the *de novo* synthesis of dNTPs.

Further clarification of the activation mechanism needs a structural approach, including X-ray crystallography. The method to overproduce this protein reported here will be useful for such analysis. In addition, the physiological role of a dNTP triphosphohydrolase activity with complicated regulation is now being examined by analyzing a TT1383 defective strain.

We thank Dr. Maria Spies for construction of the tt1383/pET11a plasmid. This work was supported in part by Grants-in-Aid for Scientific Research (13033025 to S. K. and 15570114 to R. M.) from the Ministry of Education, Science, Sports and Culture of Japan. Nucleotide sequence data are available in the DDBJ/EMBL/GenBank data bases under the accession number AB107661.

REFERENCES

1. Sissler, M., Delorme, C., Bond, J., Ehrlich, S.D., Renault, P., and Francklyn, C. (1999) An aminoacyl-tRNA synthetase paralog with a catalytic role in histidine biosynthesis. *Proc. Natl. Acad. Sci. USA* **96**, 8985–8990
2. Sekowska, A., Danchin, A., and Risler, J.L. (2000) Phylogeny of related functions: the case of polyamine biosynthetic enzymes. *Microbiology* **146**, 1815–1828
3. Miyazaki, J., Kobashi, N., Fujii, T., Nishiyama, M., and Yamane, H. (2002) Characterization of a lysK gene as an argE homolog in *Thermus thermophilus* HB27. *FEBS Lett.* **512**, 269–274
4. Oshima, T. and Imahori, K. (1974) Description of *Thermus thermophilus* (Yoshida and Oshima) comb. nov., a nonsporulating thermophilic bacterium from a Japanese thermal spa. *Int. J. Syst. Bacteriol.* **24**, 102–112
5. Yokoyama, S., Hirota, H., Kigawa, T., Yabuki, T., Shirouzu, M., Terada, T., Ito, Y., Matuo, Y., Kuroda, Y., Nishimura, Y., Kyogoku, Y., Miki, K., Masui, R., and Kuramitsu, S. (2000) Structural genomics projects in Japan. *Nat. Struct. Biol.* **7**, 943–945
6. Hoseki, J., Okamoto, A., Masui, R., Shibata, T., Inoue, Y., Yokoyama, S., and Kuramitsu, S. (2003) Crystal structure of a family 4 uracil-DNA glycosylase from *Thermus thermophilus* HB8. *J. Mol. Biol.* **333**, 515–526
7. Takeishi, S., Nakagawa, N., Maoka, N., Kihara, M., Moriguchi, M., Masui, R., and Kuramitsu, S. (2003) Crystallization and preliminary X-ray diffraction studies of nucleoside diphosphate kinase from *Thermus thermophilus* HB8. *Acta Crystallogr. D Biol. Crystallogr.* **59**, 1843–1835
8. Komori, H., Masui, R., Kuramitsu, S., Yokoyama, S., Shibata, T., Inoue, Y., and Miki, K. (2001) Crystal structure of thermostable DNA photolyase: pyrimidine-dimer recognition mechanism. *Proc. Natl. Acad. Sci. USA* **98**, 13560–13565
9. Tachiki, H., Kato, R., and Kuramitsu, S. (2000) DNA binding and protein-protein interaction sites in MutS, a mismatched DNA recognition protein from *Thermus thermophilus* HB8. *J. Biol. Chem.* **275**, 40703–40709
10. Sugahara, M., Mikawa, T., Kumasaka, T., Yamamoto, M., Kato, R., Fukuyama, K., Inoue, Y., and Kuramitsu, S. (2000) Crystal structure of a repair enzyme of oxidatively damaged DNA, MutM (Fpg), from an extreme thermophile, *Thermus thermophilus* HB8. *EMBO J.* **19**, 3857–3869
11. Nakagawa, N., Sugahara, M., Masui, R., Kato, R., Fukuyama, K., and Kuramitsu, S. (1999) Crystal structure of *Thermus thermophilus* HB8 UvrB protein, a key enzyme of nucleotide excision repair. *J. Biochem.* (*Tokyo*) **126**, 986–990
12. Seto, D., Bhatnagar, S., and Bessman, M.J. (1988) The purification and properties of deoxyguanosine triphosphate triphosphohydrolase from *Escherichia coli*. *J. Biol. Chem.* **263**, 1494–1499
13. Aravind, L. and Koonin, E.V. (1998) The HD domain defines a new superfamily of metal-dependent phosphohydrolases. *Trends Biochem. Sci.* **23**, 469–472
14. Kuramitsu, S., Hiromi, K., Hayashi, H., Morino, Y., and Kagamiyama, H. (1990) Pre–steady-state kinetics of *Escherichia coli* aspartate aminotransferase catalyzed reactions and thermodynamic aspects of its substrate specificity. *Biochemistry* **29**, 5469–5476
15. Stocchi, V., Cucchiarini, L., Canestrari F., Piacentini M.P., and Fornaini, G. (1987) A very fast ion-pair reversed-phase HPLC method for the separation of the most significant nucleotides and their degradation products in human red blood cells. *Anal. Biochem.* **167**, 181–190
16. Altschul, S.F., Gish, W., Miller, W., Myers E.W., and Lipman D.J. (1990) Basic local alignment search tool. *J. Mol. Biol.* **215**, 403–410
17. Quirk, S. and Bessman, M.J. (1991) dGTP triphosphohydrolase, a unique enzyme confined to members of the family *Enterobacteriaceae*. *J. Bacteriol.* **173**, 6665–6669

18. Quirk, S. and Do, B.T. (1997) Cloning, purification, and characterization of the *Shigella boydii* dGTP triphosphohydrolase. *J. Biol. Chem.* **272**, 332–336
19. Fersht, A.R. (1999) *Structure and Mechanism in Protein Science: A Guide to Enzyme Catalysis and Protein Folding*, Chapter 3, W.H. Freeman and Co.
20. Kierzek, R., Burkard, M.E., and Turner, D.H. (1999) Thermodynamics of single mismatches in RNA duplexes. *Biochemistry* **38**, 14214–14223
21. Peyret, N., Seneviratne, P., Allawi, H.T., and SantaLucia, J., Jr. (1999) Nearest-neighbor thermodynamics and NMR of DNA sequences with internal A.A, C.C, G.G, and T.T mismatches. *Biochemistry* **38**, 3468–3477
22. Jordan, A. and Reichard, P. (1998) Ribonucleotide reductases. *Annu. Rev. Biochem.* **67**, 71–98
23. Arner, E.S.J. and Eriksson, S. (1995) Mammalian deoxyribonucleoside kinases. *Pharmacol. Ther.* **67**, 155–186
24. Eriksson, S., Munch-Petersen, B., Johansson, K., and Eklund, H. (2002) Structure and function of cellular deoxyribonucleoside kinases. *Cell. Mol. Life Sci.* **59**, 1327–1346